[P6]

P. Suvikunnas, J. Villanen, K. Sulonen, C. Icheln, J. Ollikainen, and P. Vainikainen, "Evaluation of the performance of multiantenna terminals using a new approach," *IEEE Transactions on Instrumentation and Measurement*, vol. 55, no. 5, pp. 1804 - 1813, October 2006. 

# Evaluation of the Performance of Multiantenna Terminals Using a New Approach

Pasi Suvikunnas, Juha Villanen, Kati Sulonen, Clemens Icheln, Jani Ollikainen, *Member, IEEE*, and Pertti Vainikainen, *Member, IEEE*

***Abstract*—In this paper, an advanced experimental plane-wave-based method (EPWBM) for evaluation of the performance of multiantenna systems is considered. The method enables a statistical antenna evaluation without performing long routes of radio-channel sounder measurements to be carried out separately for each antenna under test. The EPWBM utilizes the joint contribution of the estimated signal spectrum and the simulated or measured complex three-dimensional (3-D ) radiation patterns of antennas under test. The proposed method enables more comprehensive antenna evaluation in a shorter time period compared to direct measurements. For validation purposes, the results obtained with the EPWBM are compared with the results of direct radio-channel measurements. The method is shown to be sufficiently accurate for comparing the performance of different antenna configurations. The average difference between the two methods is below 1 dB when estimating the diversity gain of two-element antennas. Further, the maximum difference between the methods in multiple-input multiple-output analysis is below 1 b/s/Hz in estimating mean capacity.**

***Index Terms*—Antenna evaluation methods, channel-estimation algorithms, diversity antenna arrangements, diversity systems, mobile antennas, mobile communication systems, multiple-input multiple-output (MIMO) antennas, multiple-input multiple-output (MIMO) systems.**

## I. Introduction

THE PERFORMANCE of multiantenna configurations at both ends of the radio link is one of the key issues in order to reach the desired high data rates of the future mobile communications systems. Mobile terminal antennas have commonly been evaluated using total radiated power, total receiver sensitivity [1], or mean effective gain (MEG) [1]–[3], which are indicators of the total received signal power for single-input single-output (SISO) systems. Antenna properties also have significant effect in more advanced mobile communications systems like single-input multiple-output (SIMO) and multiple-input multiple-output (MIMO). For these systems, the commonly used performance indicators are total received signal power, diversity gain (SIMO) [4], [5], eigenvalue spread, and capacity or mutual information (MIMO) [6], [7].

In order to obtain comprehensive results when comparing the performance of multiantenna configurations, several hundred meters of measurement routes in several types of propagation environments are needed for each prototype antenna. This is difficult both due to the large number of measurements needed, and also to restrictions imposed by the authorities on the usage of the frequency bands in which commercial communications networks are operating. It would be useful to test the performance of new multiantenna mobile terminals in real signal-propagation environments during the early simulation phase of the design process, and to verify these results later with the developed prototype antennas.

In this paper, we evaluate the accuracy of the experimental plane-wave-based method (EPWBM). The EPWBM is an extension of the earlier work in [3], where experimental estimation of MEG for single mobile terminal antennas was discussed. The method, the theory of which was introduced in [8], is based on the estimated radio-channel distribution and on the simulated or measured complex three-dimensional (3-D) radiation patterns of the multiantenna configurations. The method enables the evaluation of the antenna systems under development in a more effective and comprehensive way compared with direct measurements (DMs) by simplifying the evaluation process, saving evaluation time, and cutting costs. Naturally, synthetic channel models can be used instead of measured ones, as was proposed in [9] for MIMO channel-modeling purposes. The possibility for practical implementation of the method was first mentioned in [10], and the method was preliminarily used for ideal dipole antenna evaluation in [6]. However, the reliability analysis of the method has not been performed earlier. Therefore, in this paper, the performance of multiantenna systems is studied using two different approaches. First, antenna evaluation is performed based on the DMs, and later on, the results obtained with the EPWBM are validated based on the DM. This paper, which is the extension for [11],[1] is organized as follows. A description of the measurement system and theory related to the EPWBM is presented in Section II. The validation of the EPWBM is given in Section III. Finally, discussion and conclusions are presented in Sections IV and V, respectively.

Manuscript received June 15, 2004; revised February 27, 2006.

P. Suvikunnas, J. Villanen, C. Icheln, and P. Vainikainen are with the IDC, SMARAD/Radio Laboratory, Helsinki University of Technology, FI-02015 HUT, Finland (e-mail: pasi.suvikunnas@tkk.fi; juha.villanen@tkk.fi; icheln@tkk.fi; pertti.vainikainen@tkk.fi).

K. Sulonen is with the Academy of Finland, FI-00501 Helsinki, Finland (e-mail: kati.sulonen@aka.fi).

J. Ollikainen is with the Nokia Research Center, FI-00045 NOKIA GROUP, Helsinki, Finland (e-mail: jani.ollikainen@nokia.com).

Digital Object Identifier 10.1109/TIM.2006.873815

[1]The paper was initially presented in the proceedings of IMTC2004.

## II. Multiantenna Evaluation Methods

### A. Signal Model

In this paper, diversity analysis is performed for SIMO systems, and capacity and eigenvalue analysis is carried out for MIMO systems. Regardless of the communications system used, the instantaneous narrow-band complex channel matrix (MIMO), or vector (SIMO), or number (SISO) can be expressed by

$$\mathbf{H}^{(i)} = \begin{bmatrix} h_{1,1}^{(i)} & \cdots & h_{1,n_\mathrm{t}}^{(i)} \\ \vdots & \ddots & \vdots \\ h_{n_\mathrm{r},1}^{(i)} & \cdots & h_{n_\mathrm{r},n_\mathrm{t}}^{(i)} \end{bmatrix} \tag{1}$$

where $\mathbf{H}^{(i)}$ is realized for each measured sample of the channel $(i)$[2] by removing the noise and summing the impulse responses of the radio-channel measurements coherently in the delay domain.[3] Therefore, the number of the antennas $n_\mathrm{r}$ at the receiver (Rx) and $n_\mathrm{t}$ at the transmitter (Tx) dictates the dimensions of the matrix (1). The normalized channel matrix $\mathbf{H}_{\mathrm{norm}}^{(i)}$ is defined as

$$\mathbf{H}_{\mathrm{norm}}^{(i)} = \frac{\mathbf{H}^{(i)}}{\frac{1}{\sqrt{n_\mathrm{t} n_\mathrm{r}}} \frac{1}{2N+1} \sum_{i-N}^{i+N} \left\| \mathbf{H}_{\mathrm{ref}}^{(i)} \right\|_F} \tag{2}$$

where $\mathbf{H}_{\mathrm{ref}}^{(i)}$ is a channel matrix for normalization antennas. A notation $\| \bullet \|_\mathrm{F}$ stands for the Frobenius norm, and $2N+1$ is the number of samples over a sliding window. The matrix operation in the denominator of (2) sets the received power for the same level in the comparison of the DM and the EPWBM and mitigates a slow fading from the received signal. Basically, the reference antenna system can be selected freely in the normalization purposes. In diversity analysis, only one reference antenna was used at the receiver, whereas in the MIMO analysis, the number of the reference and investigated antennas was equal. Thus, having comparable channel matrices with the diversity and MIMO analysis, $n_\mathrm{r}$ is omitted from (2) in the diversity analysis.

### B. Diversity Analysis

In the special case of SIMO, $\mathbf{H}_{\mathrm{norm}}^{(i)}$ simplifies to a column vector, the entries of which define the instantaneous complex fields of the received signals. Thus, the instantaneous power received by the antenna branches can be defined as

$$\mathbf{P}_{\mathrm{norm}}^{(i)} = \mathbf{H}_{\mathrm{norm}}^{(i)} \circ \mathbf{H}_{\mathrm{norm}}^{*(i)} \tag{3}$$

where an asterisk stands for complex conjugate operator and $\circ$ is the elementwise (Schur–Hadamard) matrix product operator.

[2]The used measurement system enables us to take about four samples per wavelength.

[3]The EPWBM is developed only for narrowband systems at this stage.

Further, maximal ratio combined (MRC) power is simply defined by

$$P_{\mathrm{MRC}}^{(i)} = \sum_{r=1}^{n_\mathrm{r}} p_{\mathrm{r},1}^{(i)} \tag{4}$$

where $p_{\mathrm{r},1}^{(i)}$ are the entries of the vector $\mathbf{P}_{\mathrm{norm}}^{(i)}$. The samples of instantaneous branch powers $\{p_{\mathrm{r},1}^{(i)}\}_{i=1}^{N_\mathrm{s}}$ denoted by $P_{\mathrm{r},1}$, over the samples of the channel $N_\mathrm{s}$, are estimated from the measurements. The cumulative distribution function (cdf) of the branch powers can be defined in discrete form by $F(P_p) = P(P_{\mathrm{r},1} \leq P_p) = p$, where $p$ is the considered probability level. The cdfs of the branch and MRC powers are defined in the diversity analysis.

### C. MIMO Analysis

The ability of an MIMO system to utilize parallel independent channels is defined by the eigenvalues of $\mathbf{R}_{\mathrm{norm}}^{(i)} = \mathbf{H}_{\mathrm{norm}}^{(i)} \mathbf{H}_{\mathrm{norm}}^{(i)\mathrm{H}}$, denoted by $\lambda_k^{(i)}$ [12]. Here, superscript H stands for the Hermitian transpose. From physical point of view, eigenvalues, the maximum number of which is defined by $k = \min(n_\mathrm{t}, n_\mathrm{r})$, gives the number of the spatially independent channels and defines power allocation among those channels. Thus, the cdfs of the eigenvalues $\{\lambda_k^{(i)}\}_{i=1}^{N_\mathrm{s}}$ over the samples of the channel is a useful indicator of the performance of an MIMO system. Shannon has defined an upper limit for capacity in [13], and it has been extended for MIMO systems in [14]. The "instantaneous" capacity or mutual information can be defined as

$$C^{(i)} = \log_2 \left[ \det \left( \mathbf{I} + \frac{\rho}{n_\mathrm{t}} \mathbf{R}_{\mathrm{norm}}^{(i)} \right) \right] \quad [\mathrm{b/s/Hz}] \tag{5}$$

where $\rho$ is the system signal-to-noise ratio (SNR), and $\mathbf{I}$ is the identity matrix of the same size as $\mathbf{R}_{\mathrm{norm}}^{(i)}$. The number of Tx antennas $(n_\mathrm{t})$ in (5) sets the transmitted power for the same level regardless of the communications systems (SISO, SIMO). It is worth noting that (5) is basically a theoretical upper limit for the achievable capacity of the system. Although unattainable in practice, it can be considered as a useful performance indicator in the comparison of the performance of different multielement antenna systems. Therefore, in MIMO analysis, the cdf of mutual information $\{C_{\mathbf{H}}^{(i)}\}_{i=1}^{N_\mathrm{s}}$ over the samples of the channel is also used in the comparison of the methods.

### D. Direct Measurement (DM)

The wideband channel sounder used is capable of dynamic MIMO channel measurements at 2.154 GHz [15], [16]. In the measurement system, a linear or zigzag transmitting (Tx) antenna array and a spherical receiving (Rx) antenna array has been connected to a fixed transmitter and to a moving receiver of the radio-channel sounder, respectively. The Tx and Rx antenna arrays consist of identical dual-polarized patch antennas with theta- and phi-polarized feeds called VP and HP, respectively. Radiation patterns of the used dual-polarized patch antennas are presented in [15]. The directivities of the patch

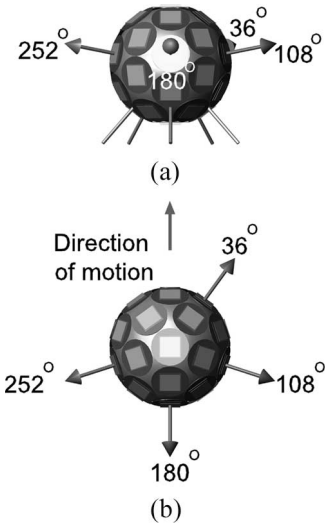


Fig. 1. Spherical Rx antenna array. The antenna element orientations used in this paper are indicated by arrows and antenna orientations relative to the direction of motion in degrees. (a) Side view. (b) Top view.

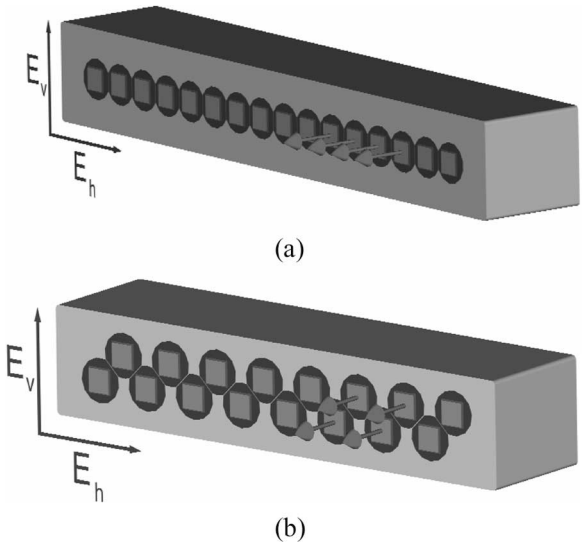


Fig. 2. Tx antenna array. The antenna elements used in this paper are indicated by arrows. (a) Linear array. (b) Zigzag array.

antennas are 7.8 dBi with 6-dB beamwidths of 90° and 100° for the E and H planes, respectively. The diameter of the spherical array is $2.37\lambda$ at 2.154 GHz, and the interelement spacing of the antenna elements depending on the neighboring element is $0.76$ or $0.85\lambda$. Further, interelement spacings of the zigzag and the linear antenna arrays are $0.5\lambda$ (in azimuth) and $0.72\lambda$, respectively. Fast switches capable of measuring a $16 \times 64$ MIMO channel matrix[4] in 9 ms are used at both ends of the link [16]. However, the transmitted power is restricted to 26 dBm due to limited power-handling capability of the p-i-n diode switch array, which limits the use of the system mainly for pico-, micro- and small macrocells. In DM, radio-channel matrices $\mathbf{H}_{\mathrm{norm}}^{(i)}$ as well as normalization matrices $\mathbf{H}_{\mathrm{ref}}^{(i)}$ are generated selecting the desired antenna element feeds from both ends of the link in order to generate different antenna system realizations. The Rx and Tx measurement antenna arrays are presented in Figs. 1 and 2, respectively. The arrows in Figs. 1 and 2 indicate the selected antenna elements in the comparison of the two methods. The orientations of the antennas on the spherical antenna are marked in degrees $(36^\circ, 108^\circ, 180^\circ, 252^\circ)$.

Measurement results obtained in three different propagation environments are considered: an indoor picocell environment in the Computer Science Building located at the campus area of Helsinki University of Technology (HUT), as well as outdoor microcell and small outdoor macrocell environments, both in the Helsinki downtown. The linear antenna array [see Fig. 2(a)] was used in the picocell, and the zigzag antenna array [Fig. 2(b)] in the other two environments. Indoor measurement was performed on the first floor of a modern office building with transmitter antenna height of 3.8 m. The receiver trolley was moved 60 m along a lobby of the building. In the microcell measurement, the transmitter was located below the rooftop level at a height of 13 m elevated by crane, pointing along the street. The trolley was moving 87 m along a cross street over an intersection. In the small macrocell measurement, the transmitter was located on the roof of the shopping center and the receiver was moving 47 m along the street on the next block. The maps of the measurement routes and the figures of the received signal distributions are given in [17]. The realistic mobile terminal antenna arrangement studied in this paper was measured in the picocell environment, as discussed later in Section III.

[4]Only eight of the 16 elements are used at the transmitter end of the link.

### *E. Experimental Plane-Wave-Based Method (EPWBM)*

The EPWBM utilizes the joint contribution of the estimate of the incident signal distribution and the complex 3-D radiation patterns of the antennas under test. In the complex signal-propagation environment, the signal is decomposed in angle and delay dimensions forming $n$ different copies of the same transmitted signal[5] due to obstacles in the signal-propagation environment. The incident signal distribution is estimated in space using a Fourier-based channel-estimation algorithm implemented for the spherical Rx antenna array (see Fig. 1). Further, delay estimation is carried out using spreading codes of different lengths depending on the signal-propagation environment. The measurement system capable of directional channel measurements is better described in [15], and its extension for MIMO is described in [16]. Every multipath component of the signal can be denoted with an $n_{\mathrm{r}} \times n_{\mathrm{t}}$ matrix

$$\mathbf{M}_x^{(i)(n)} = \begin{bmatrix} h_1^{(i)(n)}(\theta_{\mathrm{r}}, \phi_{\mathrm{r}}) & \cdots & h_{n_{\mathrm{t}}}^{(i)(n)}(\theta_{\mathrm{r}}, \phi_{\mathrm{r}}) \\ \vdots & \ddots & \vdots \\ h_1^{(i)(n)}(\theta_{\mathrm{r}}, \phi_{\mathrm{r}}) & \cdots & h_{n_{\mathrm{t}}}^{(i)(n)}(\theta_{\mathrm{r}}, \phi_{\mathrm{r}}) \end{bmatrix} \tag{6}$$

where $x = \{\theta\theta, \phi\phi\}$ consists of the theta- and phi-polarized field components[6] presented by spherical coordinates. Angles of arrivals in elevation and azimuth are denoted by $\theta_{\mathrm{r}}$ and $\phi_{\mathrm{t}}$,

[5]Incident signals are nearly plane waves in the far field.

[6]The dual-polarized microstrip antennas located on the surface of the spherical antenna group enables us to solve the fields with theta and phi polarizations.

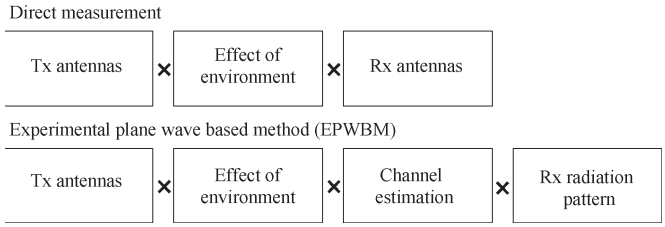


Fig. 3. Basic difference between the methods.

respectively. The radiation pattern matrix with two orthogonal polarizations is defined by

$$\mathbf{G}_y^{(n)} = \begin{bmatrix} g_1^{(n)}(\theta_{\rm r},\phi_{\rm r}) & g_1^{(n)}(\theta_{\rm r},\phi_{\rm r}) & \cdots & g_1^{(n)}(\theta_{\rm r},\phi_{\rm r}) \\ g_2^{(n)}(\theta_{\rm r},\phi_{\rm r}) & g_2^{(n)}(\theta_{\rm r},\phi_{\rm r}) & \cdots & g_2^{(n)}(\theta_{\rm r},\phi_{\rm r}) \\ \vdots & \vdots & \ddots & \vdots \\ g_{n_{\rm r}}^{(n)}(\theta_{\rm r},\phi_{\rm r}) & g_{n_{\rm r}}^{(n)}(\theta_{\rm r},\phi_{\rm r}) & \cdots & g_{n_{\rm r}}^{(n)}(\theta_{\rm r},\phi_{\rm r}) \end{bmatrix} \quad (7)$$

where $g_{n_{\rm r}}^{(n)}$ are the complex-valued 3-D far-field points of the $r$th receiver antennas, respectively, and $y$ denotes either a $\phi$- or $\theta$-polarized field component. The complex 3-D radiation patterns of the antenna configurations under test can be obtained using simulations or anechoic-chamber measurements. The gains of the antennas include dielectric, conductivity, and matching losses in (7). The antennas under test are embedded on the estimated signal distribution forming a channel matrix for the each samples of the channel by

$$\mathbf{H}^{(i)} = \sum_{n=1}^{N} \left[ \mathbf{M}_{\phi\phi}^{(i)(n)} \circ \mathbf{G}_{\phi}^{(n)} + \mathbf{M}_{\theta\theta}^{(i)(n)} \circ \mathbf{G}_{\theta}^{(n)} \right]. \quad (8)$$

Thus, the principle of the EPWBM is stated in terms of (6)–(8). While retaining the same realization of the signal distribution $\{\mathbf{M}_x^{(i)(n)}\}_{i=1}^{N_{\rm s}}$ from the channel library, test antennas can be changed to see their effect on the channel matrix sequence $\{\mathbf{H}^{(i)}\}_{i=1}^{N_{\rm s}}$. Now, for the validation of the proposed method, the same antennas that are used in DM are measured in an anechoic chamber. The results of both methods are compared using the measured radiation patterns in the EPWBM. The block diagram in Fig. 3 presents the basic difference between the EPWBM and the DM.

## III. Validation of EPWBM

### A. Diversity Analysis

Diversity gain, which is a commonly used indicator in estimating diversity performance, was used in this paper as a figure of merit for comparing the results of the DM and the EPWBM. At the transmitter, the VP feed of one of the antenna elements from the antenna array is selected (see Fig. 2). At the receiver, two different antenna configurations consisting of two antennas are considered.

1) Both the VP (Br1) and the HP (Br2) feeds are selected from a single antenna element of the spherical array.
2) Either the VP or the HP feeds are selected from two adjacent antenna elements of the spherical array.

The results were normalized, as defined in (2), and the slow fading of the signal was removed by averaging over about $25\lambda$ $(2N+1=101)$.

In Figs. 4 and 5, the cdfs of the powers received by both branches (Br1 and Br2) and the MRC power are shown for the two methods. The dotted line indicates the results of the DM and the solid line, the results of the EPWBM. In order to increase the statistical significance of the comparison, we define diversity gain in two ways: the improvement achieved when the MRC power is compared at first to the power of the Br1, and second, to the power of the Br2. In Fig. 4(a), the dual-polarized antenna element (108°) of the spherical antenna array was chosen to represent a polarization-diversity arrangement, the VP feed being the Br1 and the HP feed being the Br2. The diversity gains are defined for two probability levels: $G_{10}$ and $G_{50}$ for 10% and 50%, respectively. At the 50% probability level, only the weaker branch (Br2) is illustrated, and at the 10% probability level, only the stronger branch (Br1) is illustrated. In Fig. 4(b), the vertically polarized feeds of two adjacent antenna elements (36°) and (108°) of the spherical antenna array were chosen to represent a space-diversity arrangement. In all the studied cases, the order of the stronger and the weaker branch are the same in both methods.

A more comprehensive analysis is presented in Table I, in which the results of three different signal-propagation environments are considered. The differences between the diversity-gain values obtained with the two methods are evaluated using the formula

$$\Delta G_{p,{\rm Br}x} = G_{p,{\rm Br}x,{\rm EPWBM}} - G_{p,{\rm Br}x,{\rm DM}} \quad [{\rm dB}] \quad (9)$$

where $G$ is the diversity gain obtained with either the DM or the EPWBM. Subindex Br$x$ refers to either Br1 or Br2, and $p$ is the probability level from which the comparison is made ($p=10\%$ or $p=50\%$). In Table I, the notation Rx36°VPHP, for example, indicates that both feeds of element (36°) of the spherical antenna array are used, whereas notation Rx36°108°VP indicates that VP feeds from antenna elements (36°) and (108°) are used.

According to Table I, the average difference (over all the environments) between the predicted and the directly measured diversity-gain results lies within 0.88 dB for all the cases, which shows a good agreement between the two methods. A maximum difference of 2.64 dB is found from the picocell environment (Rx108°VPHP, Br2, 50%). The differences between the results are fairly similar in the different signal-propagation environments (picocell, microcell, macrocell) and in the different antenna configurations (VP, HP, VPHP), which means that the EPWBM performs in a relatively similar manner regardless of antenna type or signal-propagation environment.

Finally, a realistic mobile terminal antenna prototype introduced in [4] is considered. The prototype consists of two square-shaped planar-inverted F antennas (PIFAs) located on the left and right upper corners of a metallic ground plane $(\text{width} = 40 \text{ mm},\ \text{length} = 100 \text{ mm})$. The prototype was first measured in the picocell environment, and after that, evaluated with the EPWBM using the simulated complex 3-D radiation

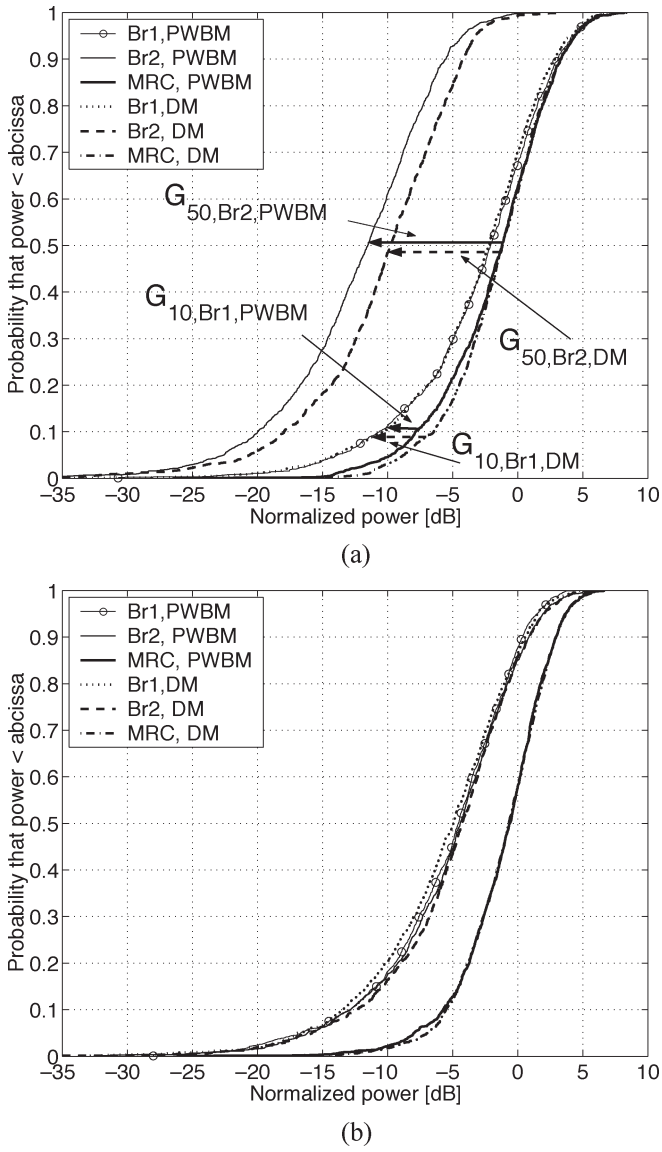


Fig. 4. Comparison of EPWBM and DM in the macrocell environment. (a) Using the VP and HP branches of the Rx element 108°. (b) Using the VP branches of the Rx elements 36° (Br1) and 108° (Br2).

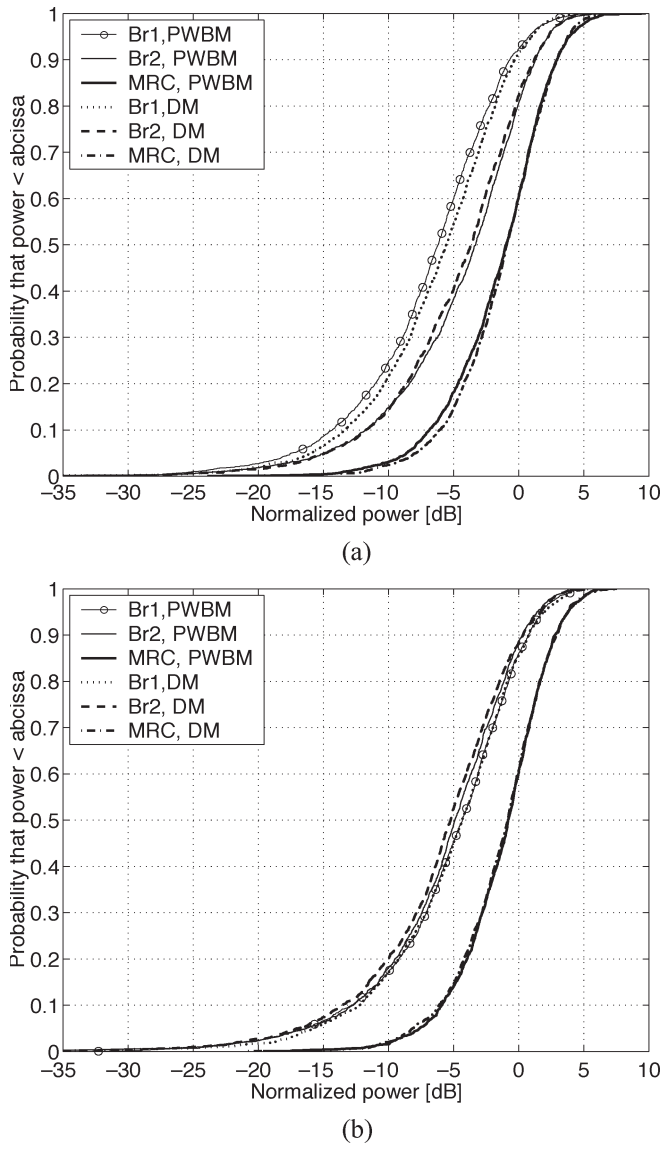


Fig. 5. Comparison of EPWBM and DM in the picocell environment with a realistic mobile terminal antenna configuration. (a) In free space. (b) Beside a head model.

patterns of the antenna configuration. Thus, two separate measurements were carried out, which have some effect on the fast fading of the signal owing to the small differences in the measurement route. However, the results can be considered statistically very reliable. Both free-space radiation patterns and radiation patterns obtained in talk position beside a phantom head model were used in the analysis. The good agreements between the results in Fig. 5(a) and (b) shows that based on the simulated radiation patterns of realistic mobile antenna prototypes, the EPWBM can provide a rather reliable estimation of diversity gain.

### *B. MIMO Analysis*

In the MIMO analysis, the cdfs of the instantaneous capacity $\{C^{(i)}\}_{i=1}^{N_s}$ (5) as well as the eigenvalues $\{\lambda_k^{(i)}\}_{i=1}^{N_s}$ of $\{\mathbf{R}_{\text{norm}}^{(i)}\}_{i=1}^{N_s}$ over the samples of the channel are used as the figures of merit for the validation of the EPWBM. Basically, two different antenna-array types are considered:

1) two (2VP) or four (4VP) VP feeds of the adjacent antenna elements from both ends of the link;
2) one HP and VP (1HP1VP) feed or two HP and VP (2HP2VP) feeds of adjacent antenna elements from both ends of the link.

In the $2 \times 2$ MIMO cases (2VP and 1HP1VP), the elements (36°) and (108°) are selected from the spherical antenna array (see Fig. 1), and in the $4 \times 4$ MIMO cases (4VP and 2HP2VP), the elements (36°), (108°), (180°), and (252°) are selected. The results obtained with the evaluated MIMO antenna configurations were normalized by averaging the received powers over the powers received by single-polarized antenna configurations 2VP or 4VP (2), according to the size of the configuration under evaluation. Slow fading was removed by performing sliding mean over about $25\lambda$, like in the diversity analysis (2). The system SNR $\rho$ in (5) was 10 dB.

TABLE I
DIFFERENCES IN THE DIVERSITY-GAIN RESULTS BETWEEN EPWBM AND DM

| $\Delta G_{p,Brx}$[dB] | Br1, 10% | Br2, 10% | Br1, 50% | Br2, 50% |
|---|---|---|---|---|
| picocell, Rx36°VPHP | -1.01 | 1.42 | 0.86 | 2.18 |
| picocell, Rx36°108°VP | 2.28 | -1.04 | 1.91 | -0.40 |
| picocell, Rx36°108°HP | 1.00 | -1.12 | 1.64 | -0.34 |
| picocell, Rx108°VPHP | -1.71 | 2.34 | -0.76 | 2.64 |
| picocell, Rx108°180°VP | 0.32 | 0.83 | -0.61 | -0.44 |
| picocell, Rx108°180°HP | 0.09 | 0.83 | -0.15 | -0.13 |
| picocell, Rx180°VPHP | -1.70 | 1.90 | -0.89 | 2.40 |
| microcell, Rx36°VPHP | -1.07 | -0.33 | -0.41 | 1.03 |
| microcell, Rx36°108°VP | 0.79 | 0.63 | 0.42 | -0.10 |
| microcell, Rx36°108°HP | -0.53 | 1.49 | -0.28 | 0.68 |
| microcell, Rx108°VPHP | -1.23 | 2.76 | -0.41 | 1.89 |
| microcell, Rx108°180°VP | -0.02 | 2.18 | 0.06 | 1.06 |
| microcell, Rx108°180°HP | 0.03 | 3.90 | -0.02 | 2.15 |
| microcell, Rx180°VPHP | -0.56 | -0.27 | -0.25 | -0.02 |
| macrocell, Rx36°VPHP | -0.81 | 1.44 | -1.01 | 0.91 |
| macrocell, Rx36°108°VP | -0.79 | 0.21 | -0.31 | 0.23 |
| macrocell, Rx36°108°HP | -0.24 | 0.34 | -0.21 | 0.53 |
| macrocell, Rx108°VPHP | -1.20 | 0.62 | -0.18 | 1.73 |
| macrocell, Rx108°180°VP | 0.46 | -1.47 | 0.11 | -0.11 |
| macrocell, Rx108°180°HP | -0.23 | 0.02 | 0.20 | 0.26 |
| macrocell, Rx180°VPHP | -2.11 | 1.70 | 0.23 | 2.14 |
| Mean difference | -0.39 | 0.88 | -0.00 | 0.87 |
| Standard deviation | 1.03 | 1.36 | 0.73 | 1.04 |

TABLE II
DIFFERENCES IN THE MEAN $(\Delta m_C)$ AND STANDARD DEVIATIONS $(\Delta\sigma_C)$ OF THE CAPACITY RESULTS BETWEEN EPWBM AND DM. ANTENNA CONFIGURATIONS 2VP AND 4VP ARE CONSIDERED

| 2×2 MIMO | Picocell | Microcell | Macrocell |
|---|---|---|---|
| $\Delta m_C$ [bit/s/Hz] | -0.25 | 0.12 | 0.27 |
| $\Delta\sigma_C$ [bit/s/Hz] | -0.03 | 0.02 | 0.05 |
| 4×4 MIMO | Picocell | Microcell | Macrocell |
| $\Delta m_C$ [bit/s/Hz] | -0.33 | 0.44 | 0.60 |
| $\Delta\sigma_C$ [bit/s/Hz] | 0.01 | 0.14 | 0.10 |

The differences between the methods in mean and standard-deviation values of $\{C^{(i)}\}_{i=1}^{N_s}$ and $\{\lambda_k^{(i)}\}_{i=1}^{N_s}$ are presented in Tables II–V for the three investigated environments. The comparison has been carried out using the expression

$$\Delta X_y = X_{y,\mathrm{EPWBM}} - X_{y,\mathrm{DM}} \tag{10}$$

where $X$ indicates either mean $(m)$ or standard deviation $(\sigma)$, and subindex $y$ refers to either mutual information $(C^{(i)})$ or eigenvalue $(\lambda_k^{(i)})$. All the values are presented in linear scale. The results for $\Delta m_C$ and $\Delta\sigma_C$ are presented in Tables II and IV for the two antenna configurations. The respective results for $\Delta m_\lambda$ and $\Delta\sigma_\lambda$ from the weakest to the strongest eigenvalue are presented in Tables III and V.

TABLE III
DIFFERENCES IN THE MEAN $(\Delta m_\lambda)$ AND THE STANDARD DEVIATIONS $(\Delta\sigma_\lambda)$ OF THE EIGENVALUE RESULTS BETWEEN EPWBM AND DM. ANTENNA CONFIGURATIONS 2VP AND 4VP ARE CONSIDERED

| 2×2 MIMO | Picocell $\lambda_2/\lambda_1$ | Microcell $\lambda_2/\lambda_1$ | Macrocell $\lambda_2/\lambda_1$ |
|---|---|---|---|
| $\Delta m_\lambda$ | -0.04/0.02 | 0.02/-0.01 | 0.05/-0.06 |
| $\Delta\sigma_\lambda$ | -0.02/0.06 | 0.03/-0.02 | 0.05/-0.14 |
| 4×4 MIMO | Picocell $\lambda_4/\lambda_3/\lambda_2/\lambda_1$ | Microcell $\lambda_4/\lambda_3/\lambda_2/\lambda_1$ | Macrocell $\lambda_4/\lambda_3/\lambda_2/\lambda_1$ |
| $\Delta m_\lambda$ | -0.01/-0.03/ -0.05/0.09 | 0.00/0.03/ 0.07/-0.09 | 0.01/0.05/ 0.11/-0.18 |
| $\Delta\sigma_\lambda$ | -0.01/-0.01/ 0.01/0.13 | 0.00/0.03/ 0.05/-0.16 | 0.01/0.03/ 0.06/-0.27 |

TABLE IV
DIFFERENCES IN THE MEAN $(\Delta m_C)$ AND THE STANDARD DEVIATIONS $(\Delta\sigma_C)$ OF THE CAPACITY RESULTS BETWEEN EPWBM AND DM. ANTENNA CONFIGURATIONS OF 1HP1VP AND 2HP2VP ARE CONSIDERED

| 2×2 MIMO | Picocell | Microcell | Macrocell |
|---|---|---|---|
| $\Delta m_C$ [bit/s/Hz] | -0.56 | -0.12 | -0.13 |
| $\Delta\sigma_C$ [bit/s/Hz] | -0.11 | 0.05 | 0.05 |
| 4×4 MIMO | Picocell | Microcell | Macrocell |
| $\Delta m_C$ [bit/s/Hz] | -0.82 | -0.09 | -0.35 |
| $\Delta\sigma_C$ [bit/s/Hz] | -0.06 | -0.11 | -0.01 |

TABLE V
DIFFERENCES IN THE MEAN $(\Delta m_\lambda)$ AND THE STANDARD DEVIATIONS $(\Delta\sigma_\lambda)$ OF THE EIGENVALUE RESULTS BETWEEN EPWBM AND DM. ANTENNA CONFIGURATIONS OF 1HP1VP AND 2HP2VP ARE CONSIDERED

| 2×2 MIMO | Picocell $\lambda_2/\lambda_1$ | Microcell $\lambda_2/\lambda_1$ | Macrocell $\lambda_2/\lambda_1$ |
|---|---|---|---|
| $\Delta m_\lambda$ | -0.06/-0.19 | -0.01/0.00 | 0.00/-0.08 |
| $\Delta\sigma_\lambda$ | -0.06/-0.00 | 0.01/0.09 | -0.01/0.00 |
| 4×4 MIMO | Picocell $\lambda_4/\lambda_3/\lambda_2/\lambda_1$ | Microcell $\lambda_4/\lambda_3/\lambda_2/\lambda_1$ | Macrocell $\lambda_4/\lambda_3/\lambda_2/\lambda_1$ |
| $\Delta m_\lambda$ | -0.01/-0.05/ -0.08/-0.29 | -0.00/0.00/ -0.02/-0.07 | -0.00/-0.01/ -0.03/-0.10 |
| $\Delta\sigma_\lambda$ | -0.01/-0.02/ -0.00/-0.12 | -0.00/0.00/ -0.01/-0.06 | -0.00/0.00/ -0.01/-0.07 |

Considering all the environments, the largest differences between the methods are found from the results of the 2HP2VP MIMO system in the picocell environment (see Tables IV and V). The largest difference in mean capacity $(\Delta m_C)$ is

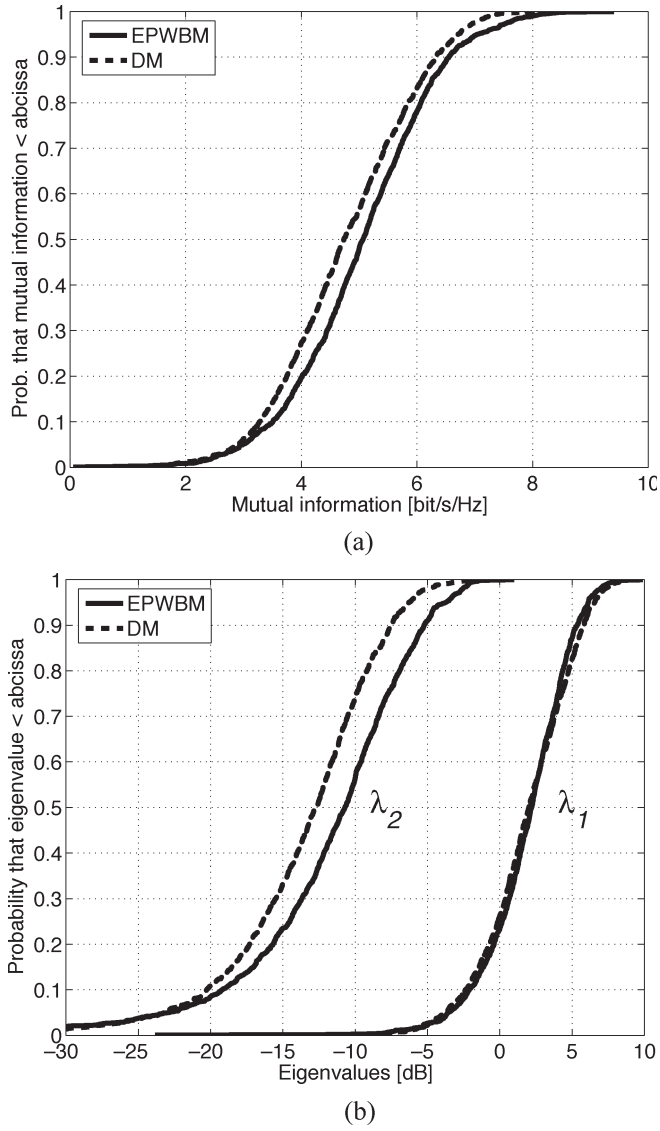


Fig. 6. Comparison of EPWBM and DM in the 2VP case. (a) cdfs of the instantaneous capacity (mutual information). (b) cdfs of the powers of two eigenvalues ($\lambda_1$ and $\lambda_2$).

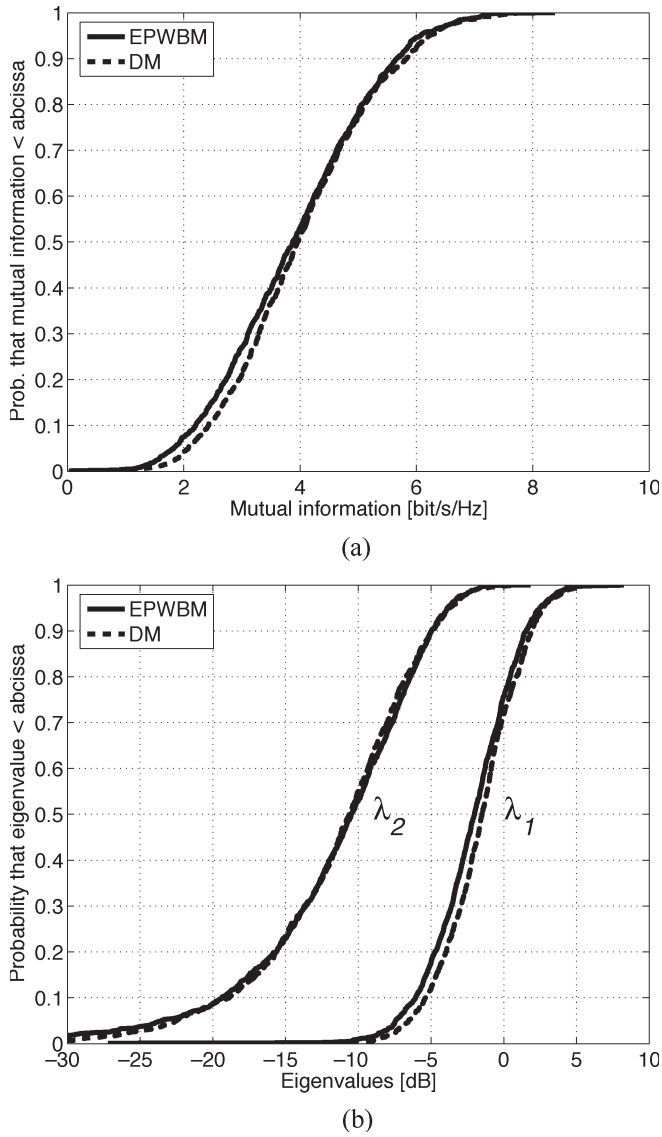


Fig. 7. Comparison of EPWBM and DM in the 1HP1VP case. (a) cdfs of the instantaneous capacity (mutual information). (b) cdfs of the powers of two eigenvalues ($\lambda_1$ and $\lambda_2$).

0.82 b/s/Hz, whereas the largest differences in mean of the eigenvalues $(\Delta m_\lambda)$ are 0.01, 0.05, 0.08, and 0.29 from the weakest $(\lambda_4)$ to the strongest eigenvalue $(\lambda_1)$. Further, the largest differences in standard deviations of the eigenvalues $(\Delta\sigma_\lambda)$ are 0.01, 0.02, 0.00, and 0.12, respectively.

A more detailed analysis is presented for the small macrocell environment. The cdfs of $\{C^{(i)}\}_{i=1}^{N_s}$ and $\{\lambda_k^{(i)}\}_{i=1}^{N_s}$ for the 2VP and 1HP1VP cases are presented in Figs. 6 and 7, respectively. The respective results for the 4VP and 2HP2VP cases are presented in Figs. 8 and 9, respectively. Dotted and solid lines present the results of the DM and the EPWBM, respectively. The best agreement between the two methods (in macrocell) is achieved in the 1HP1VP case (Fig. 7), but the difference of the 2VP results is also insignificant (Fig. 6). In the small macrocell environment, the largest difference between the eigenvalue results of the two methods can be found from the 4VP case.

## IV. Discussion

The EPWBM has proven to be sufficiently accurate to be used in the comparison of the performance of multiantenna configurations. Using the EPWBM, the performance of a multiantenna system can effectively be evaluated in several propagation environments. Antennas can be rotated in azimuth and also in elevation direction easily to get a comprehensive insight into the antenna characteristics, which is a useful property, e.g., in MEG [3], MRC MEG [4], and MELG [18] analysis. Lets consider a situation where $N_a$ different antenna prototypes should be evaluated in $N_l$ different usage positions[7] and in $N_c$ different environments. Thus, the total number of the measurements needed by traditional means would be $N_a \times N_l \times N_c$. However, by using the EPWBM, the number of the needed measurements drops to $N_c$ since the antenna implementation

[7]A user can hold a mobile phone in numerous azimuth and elevation positions.

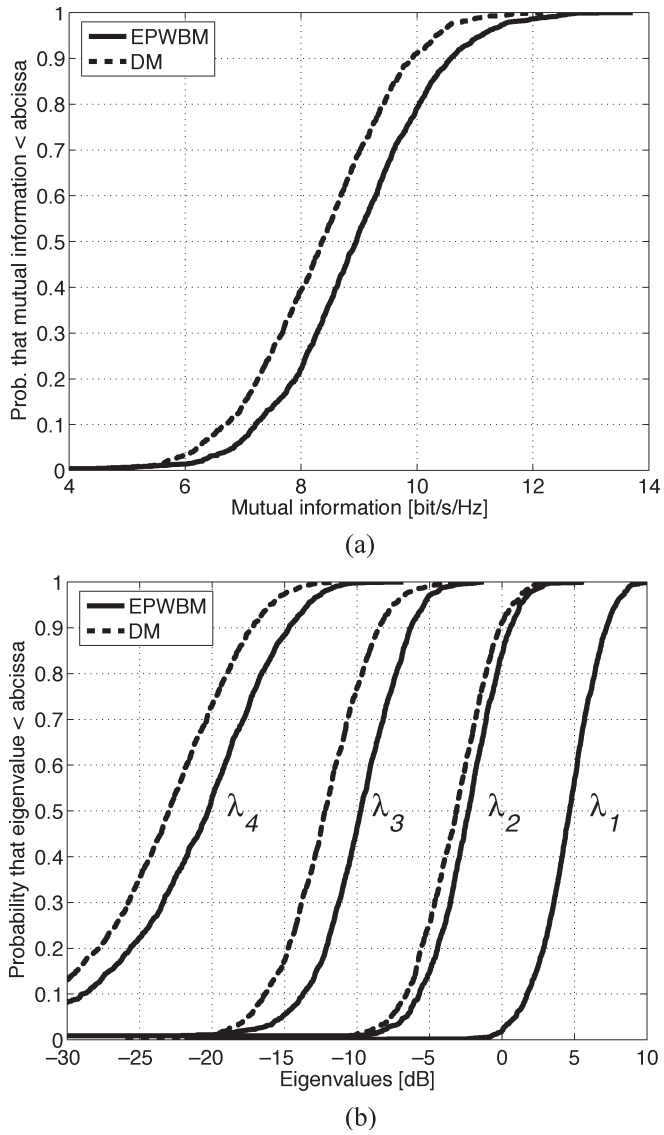


Fig. 8. Comparison of EPWBM and DM in the 4VP case. (a) cdfs of the instantaneous capacity (mutual information). (b) cdfs of the powers of four eigenvalues ($\lambda_1$, $\lambda_2$, $\lambda_3$, and $\lambda_4$).

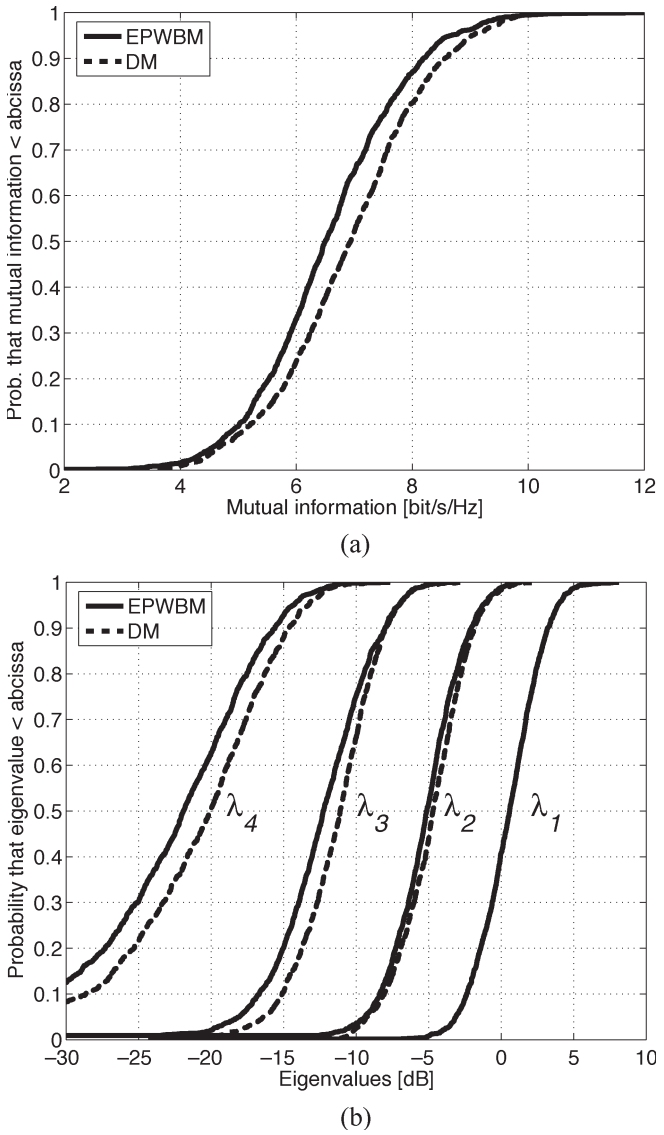


Fig. 9. Comparison of EPWBM and DM in the 2HP2VP case. (a) cdfs of the instantaneous capacity (mutual information). (b) cdfs of the powers of four eigenvalues ($\lambda_1$, $\lambda_2$, $\lambda_3$, and $\lambda_4$).

and rotation can be done computationally afterwards. Hence, the time saving is remarkable compared to DM. Further, multiantenna systems can be tested already during the design process, even before a prototype antenna is constructed using the simulated radiation patterns and the previously measured channel library. Further, the radio channel stays exactly the same for all antenna configurations under test, which partly compensates the inaccuracy of the method discussed next.

The spherical antenna array used in this paper is a feasible antenna-array structure for channel estimation with this given number of antenna elements [15]. Especially, the accuracy in the elevation-angle estimation is better compared to planar-type antennas due to the spherical shape of the measurement antenna array. Further, the accuracy in the azimuth-angle estimation is almost constant. However, the limitations of the beamforming algorithm, and any other signal estimation algorithm as well, in estimating the details of the scattering field, are caused by the physical restrictions of the measurement system used. The estimation of the weaker signals deteriorates in highly scattering environments because of restrictions in channel estimation. From the antenna point of view, an infinite size of antenna array with infinite number of elements would be needed to fulfill a perfect accuracy requirement. Further, measurement errors are always present in all kinds of measurements. Nevertheless, the results are shown to be statistically reliable.

In order to achieve reliable results in channel estimation, there should not be scatterers too close to the receiver antenna array, and the antennas under test should be smaller in size than the spherical antenna array used in the channel estimation. This basically means that according to the estimation theory, the far-field assumption should also be valid in channel estimation; otherwise, the estimation result deteriorates. In the far field, the signals received by an antenna can locally be considered to be plane waves, and the used Fourier-based estimation algorithm

estimates more dominant signal components properly. Near-field conditions are exceptional even in the picocell environment for the used frequency range of 2.154 GHz, which is evident based on the similarity of the picocell results compared to the results of the other environments.

A more advanced channel-estimation algorithm, like Space-Alternating Generalized Expectation Maximization (SAGE) [19], is under consideration in order to improve the results. However, the accuracy of antenna calibration is a critical issue in more advanced channel-estimation algorithms [20]. The final goal is to realize double directional channel estimation, which enables simultaneous antenna evaluations at both ends of the link.

## V. Conclusion

In this paper, the results of the EPWBM were compared with the DM results. The diversity performance of several multi-antenna configurations and the performance of the $2 \times 2$ and $4 \times 4$ MIMO systems were studied. The diversity-gain values as well as the mutual-information values and eigenvalues estimated by the EPWBM agree well with the DM results. Thus, the method is shown to be statistically reliable for the evaluation of different antenna systems in mobile communications.

## Acknowledgment

The authors would like to thank the following persons for their work related to this paper: J. Kivinen for the development of the measurement system; K. Kalliola and H. Laitinen for the construction of the spherical array and implementation of the beamforming algorithm; and E. Kahra for making the figures of the measurement arrays.

## References

[1] G. F. Pedersen, J. O. Nielsen "Radiation pattern measurements of mobile phones next to different head phantoms," in *Proc. IEEE 56th Veh. Technol. Conf.—Fall* 2000, vol. 4, pp. 2465–2469.

[2] T. Taga, "Analysis for mean effective gain of mobile antennas in land mobile radio environments," *IEEE Trans. Veh. Technol.*, vol. 39, no. 2, pp. 117–131, May 1990.

[3] K. Sulonen and P. Vainikainen, "Performance of mobile phone antennas including effect of environment using two methods," *IEEE Trans. Instrum. Meas.*, vol. 52, no. 6, pp. 1859–1864, Dec. 2003.

[4] J. Villanen, P. Suvikunnas, K. Sulonen, C. Icheln, J. Ollikainen, and P. Vainikainen, "Advances in diversity performance analysis of mobile terminal antennas," in *Proc. Int. Symp. Antennas Propag.*, 2004, pp. 649–652.

[5] B. M. Green and M. A. Jensen, "Diversity performance of dual-antenna handsets near operator tissue," *IEEE Trans. Antennas Propag.*, vol. 48, no. 7, pp. 1017–1024, Jul. 2000.

[6] K. Sulonen, P. Suvikunnas, L. Vuokko, J. Kivinen, and P. Vainikainen, "Comparison of MIMO antenna configurations in picocell and microcell environments," *IEEE J. Sel. Areas Commun.*, vol. 21, no. 5, pp. 703–712, Jun. 2003.

[7] D. Chizhik, J. Ling, P. W. Wolniansky, R. A. Valenzuela, N. Costa, and K. Huber, "Multiple-input—Multiple-output measurements and modeling in Manhattan," *IEEE J. Sel. Areas Commun.*, vol. 21, no. 3, pp. 703–712, Apr. 2003.

[8] Y. S. Yeh, "Antennas and polarization effects," in *Microwave Mobile Communications*, W. C. Jakes, Ed. New York: Wiley, 1974, ch. 3, p. 642.

[9] H. Xu, D. Chizhik, and R. Valenzuela, "Wave based wideband MIMO channel modeling technique," in *Proc. 13th IEEE Int. Symp. Pers., Indoor, Mobile Radio Commun.*, 2002, vol. 4, pp. 1626–1630.

[10] J. Kivinen, P. Suvikunnas, L. Vuokko, and P. Vainikainen, "Experimental investigations of MIMO propagation channels," in *Proc. IEEE Int. Symp. Antennas Propag.*, 2002, vol. 3, pp. 206–209.

[11] P. Suvikunnas, K. Sulonen, J. Villanen, C. Icheln, and P. Vainikainen, "Evaluation of performance of multi-antenna terminals using two approaches," in *Proc. IEEE Instrum. Meas. Technol. Conf.*, 2004, vol. 2, pp. 1091–1096.

[12] J. B. Andersen, "Antenna arrays in mobile communications: Gain, diversity, and channel capacity," *IEEE Antennas Propagat. Mag.*, vol. 42, no. 2, pp. 12–16, Apr. 2000.

[13] C. E. Shannon, "A mathematical theory of communications: Parts I and II," *Bell Syst. Tech. J.*, vol. 27, pp. 379–423, 1948. 623–656.

[14] G. J. Foschini, "Layered space-time architecture for wireless communication in a fading environment when using multi-element antennas," *Bell Labs Tech. J.*, vol. 1, no. 2, pp. 41–59, 1996.

[15] K. Kalliola, H. Laitinen, L. Vaskelainen, and P. Vainikainen, "Real-time 3-D spatial-temporal dual-polarized measurement of wideband radio channel at mobile station," *IEEE Trans. Instrum. Meas.*, vol. 49, no. 2, pp. 439–448, Apr. 2000.

[16] J. Kivinen, P. Suvikunnas, D. Perez, C. Herrero, K. Kalliola, and P. Vainikainen, "Characterization system for MIMO channels," in *Proc. 4th Int. Symp. Wireless Pers. Multimedia Commun.*, 2001, pp. 159–162.

[17] K. Sulonen, P. Suvikunnas, J. Kivinen, L. Vuokko, and P. Vainikainen, "Study of different mechanisms providing gain in MIMO systems," in *Proc. IEEE 58th Veh. Technol. Conf.—Fall*, 2003, vol. 1, pp. 352–356.

[18] P. Suvikunnas, J. Salo, and P. Vainikainen, "Comparison of MIMO antennas: Performance measures and evaluation results of two $2 \times 2$ antenna configurations," in *Proc. Nord. Radio Symp.*, 2004.

[19] K. I. Pedersen, B. H. Fleury, and P. E. Mogensen, "High resolution of electromagnetic waves in time-varying radio channels," in *Proc. 8th IEEE Int. Symp. Pers., Indoor, Mobile Radio Commun.*, 1997, vol. 2, pp. 650–654.

[20] R. S. Thoma, D. Hampicke, A. Richter, G. Sommerkorn, A. Schneider, U. Trautwein, and W. Wirnitzer, "Identification of time-variant directional mobile radio channels," *IEEE Trans. Instrum. Meas.*, vol. 49, no. 2, pp. 357–364, Apr. 2000.

**Pasi Suvikunnas** was born in Tuusula, Finland, in 1967. He received the B.Sc. degree in technology from the Technical Institute of Helsinki, Finland, in 1994 and the M.Sc. and Licentiate of Science degrees in technology from Helsinki University of Technology (HUT), Finland, in 1999 and 2002, respectively. He is currently working toward the Ph.D. degree in technology.

Since 1999, he has been with the Radio Laboratory of HUT as a Researcher. His current fields of interest are multielement antennas and mobile radio propagation.

**Juha Villanen** was born in Helsinki, Finland, in 1979. He received the M.Sc. degree in electrical engineering from Helsinki University of Technology (TKK), Espoo, Finland, in 2003. He is currently working toward the Doctorate degree at TKK.

Since 2002, he has worked as a Research Engineer at the Radio Laboratory of TKK. His research interests include design and implementation techniques of low-volume mobile terminal antennas, especially coupling-elements-based antenna structures.

**Kati Sulonen** was born in Helsinki, Finland, in 1973. She received the M.Sc., Licentiate of Science, and Ph.D. degrees in technology from Helsinki University of Technology (HUT), Finland, in 1999, 2001, and 2004, respectively, all in electrical engineering.

From 1995 to 1998, she was with Siemens Finland. From 1998 to 2004, she worked at the Radio Laboratory, HUT, as a Researcher. Currently, she is with the Academy of Finland, Helsinki, Finland. Her research interests are on the evaluation of the performance of mobile terminal antennas.

**Clemens Icheln** was born in Hamburg, Germany, in 1968. He received the M.Sc. degree in electrical engineering at Hamburg-Harburg University of Technology, Hamburg, Germany, in 1996, and the Licentiate degree in radio engineering and the Doctor of Science in technology degree from Helsinki University of Technology (TKK), Espoo, Finland, in 1999 and 2001, respectively.

He is currently working as a leading scientist at the SMARAD/Radio Laboratory of TKK. He has experience in the fields of design of mobile terminal antennas and their evaluation methods.

**Jani Ollikainen** (M'03) was born in Lahti, Finland, in 1971. He received the Master of Science in technology, Licentiate of Science in technology, and Doctor of Science in technology degrees in electrical and communications engineering in 1997, 2000, and 2004, respectively, from Helsinki University of Technology (TKK), Espoo, Finland.

From 1996 until 2003, he worked as a Researcher at the Radio Laboratory of TKK. In early 2003, he joined Nokia Research Center, Helsinki, Finland, where he is currently a Research Manager. His research interests include design, implementation, and measurement techniques of small antennas for personal mobile communications.

**Pertti Vainikainen** (S'84–S'87–M'90) received the Master of Science in technology, Licentiate of Science in technology, and Doctor of Science in technology degrees from Helsinki University of Technology (HUT), Helsinki, Finland, in 1982, 1989, and 1991, respectively.

From 1992 to 1993, he was Acting Professor of Radio Engineering, since 1993 Associate Professor of Radio Engineering, and since 1998 Professor of Radio Engineering, all at the Radio Laboratory of HUT. In 1993–1997, he was the Director of the Institute of Radio Communications (IRC) of HUT, and in 2000, he was a Visiting Professor at Aalborg University, Aalborg, Denmark. His main fields of interest are antennas and propagation in radio communications and industrial measurement applications of radio waves. He is the author or coauthor of six books and about 230 refereed international journals or conference publications and is the holder of seven patents.